Analysis of the Relationship between the Parameters of IPT Transformer and Power Electronic System

Sampath Jayalath[1] and Azeem Khan[1]
[1]University of Cape Town, South Africa
Email: sampath.jayalath@ieee.org; azeem.khan@uct.ac.za

***Abstract*—Inductive power transfer (IPT) is a promising technology that can replace the wire based power transfer. Efficiency of these systems will be a critical performance index that will determine their future in commercial applications. This paper analyses a series-series(SS) compensated IPT system using Boucherot bridge current source model to establish the relationship between magnetic pad parameters (mutual inductance) and power electronic system parameters (input and output voltages and currents). Analysis was used to design a 3.7 kW IPT system. The design is validated with the aid of finite element analysis software, ANSYS Maxwell and Simplorer. The proposed design is capable of transferring power at an efficiency of 95.88%. Furthermore, analysis shows that the mutual inductance requirement decreases with the increase in rated power for a SS compensated IPT system.**

***Index Terms*— Boucherot bridge current source model, electric vehicles, finite-element modelling, inductive power transfer, series-series compensation.**

I. Introduction

Wireless power transfer technology has become one of the emerging technologies of 21st century which has applications in consumer electronics, auto-mobiles and medical industry [1]. The important performance indices of an IPT system are power transfer efficiency, transfer power and load variation characteristics [2]. Magnetic pads and power electronics system design stages play an important role in achieving these performance indices [2],[3].

Magnetic pads with different shapes and configurations are proposed and optimized to improve the quality and coupling coefficient of the pad while limiting the leakage magnetic flux according to the limits defined under ICNIRP [4],[5]. Power electronic system design includes selection of compensation topologies [6], different switching schemes to minimize losses [8], control methods to improve the aforementioned performance indices [9].

However, most of the proposed solutions in literature follow a design procedure that separates magnetic pads design stage from power electronics design stage and fail to identify the relationship between the parameters of the magnetic pad design such as mutual inductance, coupling coefficient with the power electronics system parameters such as input to output voltage and current ratios. As a result, the system may fail to ensure maximum efficiency. Therefore, it is important to analyze the relationship between these parameters to identity the parameters that contributes to maximize efficiency.

This paper analyses the IPT system using Boucherot Bridge-Based Current Source Model to establish the basic relationship between the magnetic pad's parameters with the input voltage and output current of the system. Then the model is applied to a SS compensated topology to derive the conditions to maximize the power transmission efficiency. The design procedure derived from analysis was applied to a 3.7 kW IPT system for electric vehicles.

In addition, the analysis is extended for high power IPT systems to identify the behavior of parameters with the increase in rated power.

II. System Modelling

The analysis of maximum efficiency of an IPT system is based on Boucherot Bridge-Based Current Source Model (BBBSCM) [10]. The basic Boucherot Bridge model is shown in Fig. 1. It can be used to realize a current source at a given frequency, if $Z_a+Z_b=0$. At this condition current flowing through the Z_c depends on the source voltage and the impedance Z_a. Total impedance of the circuit is zero at resonant frequency. Therefore, in order to achieve $Z_a+Z_b=0$, Z_a can be replaced by a capacitor while the Z_b by an inductance as shown in Fig 1(b). Fig. 2 represents a loosely coupled transformer model used for an IPT system.

When comparing Fig. 1(a) and Fig. 2, L_M of the left side branch and middle leg L_M corresponds to Z_a and Z_b. Therefore, the transformer including the mutual inductance as shown by the enclosed region of Fig. 2 behave as a current source block, which results in a simplified circuit as shown in Fig. 2.

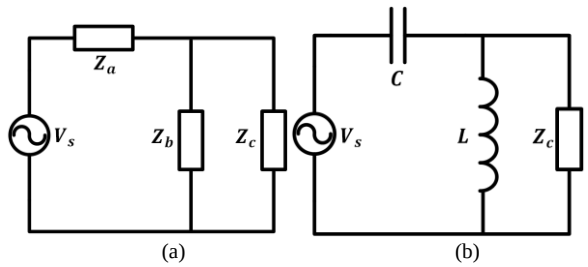

Fig. 1. Boucherot bridge current source model (a) Basic BBCSM (b) Circuit under resonance condition.

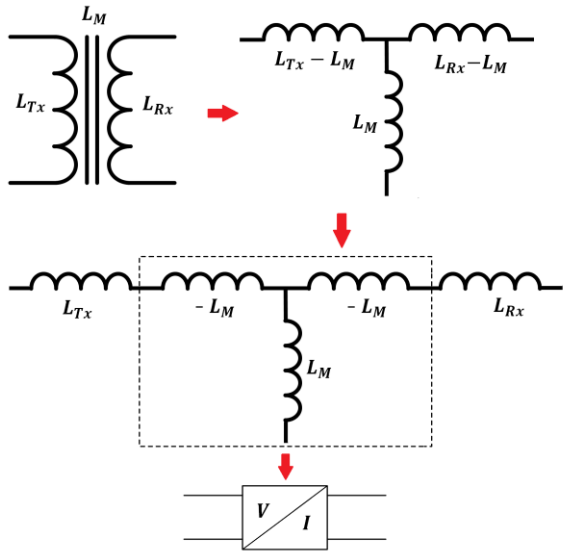

Fig. 2. Transformer model.

Therefore, output current of the current source is independent of load connected at the resonant frequency and it is given by

$$I = \frac{V_S}{(-j\omega L_M)} \tag{1}$$

According to the BBBSCM, frequency dependency of the transformer is governed by inductors L_{Tx} and L_{Rx}. In order to facilitate active flow of power, input impedance of the transformer as seen by the transmitter (T_x) side power converter should be zero [2]. This can be achieved by utilizing a capacitor either in series or parallel with the inductance of the IPT transformer. Given the high leakage inductance of IPT transformer, in order to achieve higher transmission efficiency the receiving side of the transformer is also compensated with a capacitor connected in parallel or series [2].

Fig. 3 shows the basic block diagram of an IPT system, which consists of input side DC source ($V_{dc(1)}$) or an AC-DC converters with power factor corrections to realize the dc-link. The required high frequency ac voltage is realized by a DC to AC converter. Power transferred at high frequency to the receiver-side pass through a rectifier before feeding it to the load. The analysis uses series-series compensation topology as shown in Fig.3. However, it can be applied for the other compensation topologies as well. The reactance looking from the power source is independent of either coupling coefficient or load resistance and there is no power reflection from R_x-side to T_x-side at the resonance frequency. As seen from the Fig. 3, in order to ensure the input voltage of transformer model derived from Boucherot Bridge model equal to that of the source and to achieve required power flow, the compensation capacitors of transmitter-side (T_x) and receiver-side (R_x) are given by

$$C_i = \frac{1}{\omega_T^2 L_i} \tag{2}$$

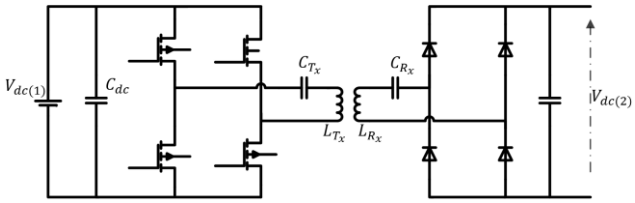

Fig. 3. Inductive power transfer system.

Where i=1, 2 stands for T_x and R_x side and L and ω are the inductance of the pad and resonance frequency of the IPT system respectively. Therefore, the load current flowing in a fully compensated IPT system according to (1)

$$I_L = -\frac{V_S}{(j\omega L_M)} \tag{3}$$

In a practical application, the output voltage of the inverter, input voltage of the T_x transformer and input voltage of the receiving side rectifier takes a rectangular form. The voltage takes the following form [2]

$$V_{i(n)} = \frac{4}{\pi}\frac{V_{dc(i)}}{n}\sin(n\pi f t_{on}) \tag{4}$$

Where i=1, 2 stands for T_x and R_x side voltages respectively. Where V_{dc}, n, f and t_{on} are dc bus voltage, odd harmonic number, frequency of operation of IPT system and on time of the pulse respectively. Furthermore as shown in [2], the harmonics of (4) are relatively small compared to the fundamental component and the full-bridge can be approximated as a sinusoidal voltage source with fundamental component

$$V_i = \frac{4V_{dc(i)}}{\pi}\sin(\pi f t_{on}) \tag{5}$$

Where i=1, 2 stands for T_x and R_x side fundamental voltages respectively. Fundamental component of current in the R_x is in phase with output voltage due to resonance phenomena. Therefore, for a series-series compensated IPT, the load circuit associated with ac-dc rectifier for a constant power delivery for a given output voltage can be modelled as a simple equivalent resistance given by

$$R_L = \frac{8}{\pi^2}\frac{V_{dc(2)}^2}{P_2} \tag{6}$$

The load matching factor can be defined as

$$f_L = \frac{R_L}{\omega L_{Rx}} \tag{7}$$

It is shown in [2], optimum value of (7) for minimum losses when considering the IPT transformer will be

$$f_{L,o} = \frac{1}{Q_{Rx}}\sqrt{1 + k^2 Q_{Tx} Q_{Rx}} \quad (8)$$

Where Q_{Tx} and Q_{Rx} are individual quality factors of transmitter and receiver. For higher values of Q_{Tx} and Q_{Rx}, $f_{L,o}$ can be further simplified to

$$f_{L,o} \approx k \quad (9)$$

Therefore, comparing (7) and (9), in order to achieve highest transmission efficiency, L_{Rx} will be approximately

$$L_{Rx} = \frac{R_L}{\omega k} \quad (10)$$

At the optimal load matching factor, the maximum efficiency of the system will be

$$E_{max} = \frac{k^2 Q_{Tx} Q_{Rx}}{\left(1+\sqrt{1+k^2 Q_{Tx} Q_{Rx}}\right)^2} \quad (11)$$

However, with misalignment value of k can degrade severely, violating the above design criteria. Furthermore, once the R_L is known, output current I_L can also be computed as

$$I_L = \sqrt{\frac{P_2}{R_L}} \quad (12)$$

By comparing (3) and (12)

$$V_s = -(j\omega L_M)\left(\sqrt{\frac{2P_2}{R_L}}\right) \quad (13)$$

The ratio between the output voltages to input voltage is given by

$$G = \frac{V_o}{V_s} = -\frac{R_L}{j\omega_0 L_M} = -\frac{R_L}{j\omega_0 k_0 \sqrt{L_{Tx} L_{Rx}}} = \frac{1}{jk_0 Q_E}\sqrt{\frac{L_{Rx}}{L_{Tx}}} \quad (14)$$

According to (14), smaller L_M and k_0 result in higher voltage gain. However, the selection of k_0 depends on the other design considerations such as limitations on transmitter and receiver side current harmonics, bifurcation and frequency splitting phenomena [11].

III. Simulation Results

The mathematical accuracy of the analysis is validated with a 3.7 kW IPT system. The system parameters are listed under Table I. Standard TIR J2954 limits the operating frequency of EV vehicles to the frequency range 81.38 kHz to 90 kHz [12]. Therefore, this paper considers 85k Hz to be the switching frequency. Charging voltage of batteries used in EVs are around 405 V for mid-power range applications, which can be represented by $V_{dc(2)}$ in (5). Therefore, $V_2 \approx$ 516 according to (5). The input side voltage $V_s = V_1$ can be computed using (13).

The magnetic pad corresponding to the required mutual in-

TABLE I
WPT System Parameters

Parameter	Value
Output power (P)	3700 W
Input dc link voltage ($V_{dc(1)}$)	432 V
Output dc link voltage ($V_{dc(2)}$)	405 V
Equivalent resistance (R_L)	35. 93 Ω
Mutual inductance (M_i)	71.83 µH
Number of turns (N)	17
Measured V_2 /I_L	505 V/ 14.05 A
Gain (G) (theoretical)	0.9366
Gain (G) (simulations)	0.9172

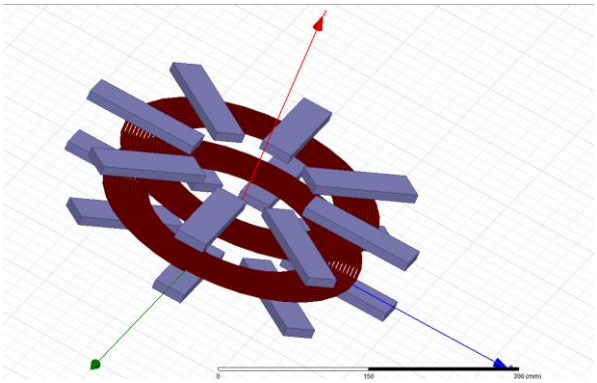

Fig. 4. Transformer (transmitter and receiver coils) model.

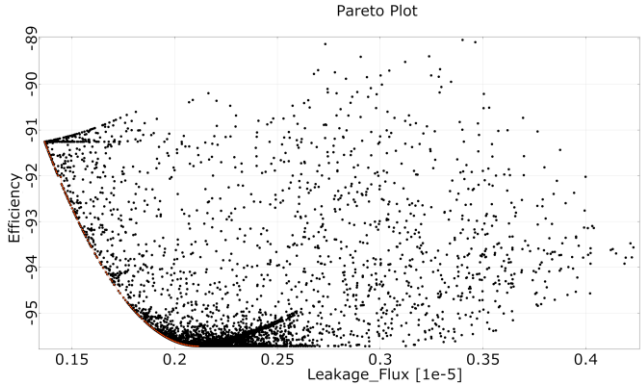

Fig. 5. Pareto-front of the optimized magnetic pad.

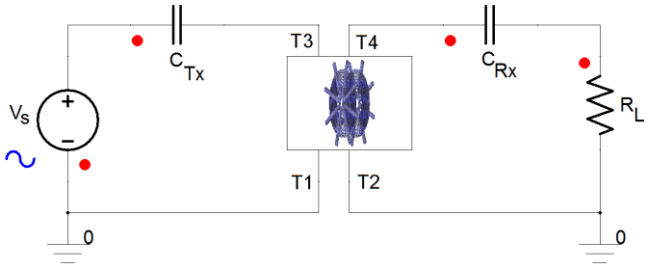

Fig. 6. Simulated IPT system in ANSYS Simplorer.

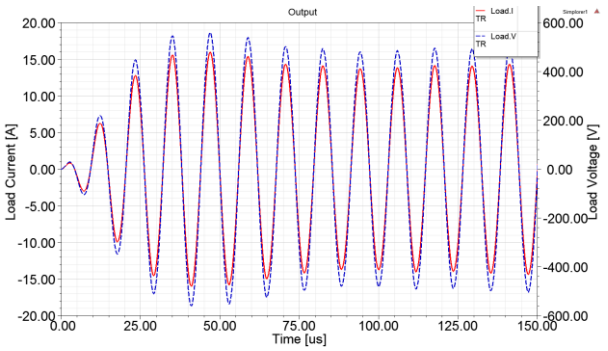

Fig. 7. Receiver-side current and voltage waveforms of the IPT system.

ductance to ensure maximum efficiency is realized with the aid of finite element analysis software ANSYS Maxwell as shown in Fig. 4. The magnetic pads are optimized using pareto-optimization strategy to maximize the coil to coil efficiency while reducing the leakage magnetic fields to the limits defined under ICNIRP [5]. Fig. 5 shows the pareto-front derived through optimization. Magnetic pad design is coupled with ANSYS Simplorer software to simulate the IPT system with the parameters listed under table I.

Fig. 6 shows the basic circuit diagram of the simulated system where input voltage source is approximated as a sinusoidal source according to (5). Fig. 7 shows the output voltages and currents of the IPT system and their corresponding peak values are listed under table I. The calculated efficiency of the system is 95.88%.

The analysis is extended for high power IPT systems to estimate the variation of the mutual inductance with the increase in rated power. Input and output dc voltages are maintained constant and SS compensation topology is used for all the design examples listed under Table II. The results show that for a series-series compensated IPT system, the required mutual inductance decreases with the increase in rated power. Therefore, as the rated power increases, the size of the resulting power pad will be small compared to low rated IPT systems. It is mainly due to the increase in flux density of the transmitter pad with the increase in rated current.

TABLE II
COMPARISON OF DIFFERENT POWER LEVELS

Power (kW)	R_L(Ω)	L_M(μH)
3.7	35.93	71.83
7.7	17.27	34.52
11	12.08	24.15
22	6.04	12.08

IV. CONCLUSION

This paper presented an analysis on the IPT system parameters based on the BBBSCM to determine the relationship between the parameters of the magnetic pad and the power electronic (PE) system. The analysis identified the importance of matching the parameters of the magnetic pad with parameters of the PE system to maximize the efficiency. Furthermore, the design procedure is applied for different rated power systems. As the rated power of the IPT system increases, the required mutual inductance decreases. It also implies that the size of the magnetic pads can be reduced with high power systems.

ACKNOWLEDGMENT

This work was supported by University of Cape Town and National Research Foundation of South Africa.

REFERENCES

[1] S. Y. R. Hui, W. Zhong and C. K. Lee, "A Critical Review of Recent Progress in Mid-Range Wireless Power Transfer," in IEEE Transactions on Power Electronics, vol. 29, no. 9, pp. 4500-4511, Sept. 2014.

[2] R. Bosshard, J. W. Kolar, J. Mühlethaler, I. Stevanović, B. Wunsch and F. Canales, "Modeling and $eta $ - $alpha $ -Pareto Optimization of Inductive Power Transfer Coils for Electric Vehicles," in IEEE Journal of Emerging and Selected Topics in Power Electronics, vol. 3, no. 1, pp. 50-64, March 2015.

[3] J. P. K. Sampath, A. Alphones and D. M. Vilathgamuwa, "Figure of Merit for the Optimization of Wireless Power Transfer System Against Misalignment Tolerance," in IEEE Transactions on Power Electronics, vol. 32, no. 6, pp. 4359-4369, June 2017.

[4] M. Lu and K. D. T. Ngo, "A Fast Method to Optimize Efficiency and Stray Magnetic Field for Inductive-Power-Transfer Coils Using Lumped-Loops Model," in IEEE Transactions on Power Electronics, vol. 33, no. 4, pp. 3065-3075, April 2018.

[5] International Commission on Non-Ionizing Radiation Protection, "ICNIRP guidelines for limiting exposure to time-varying electric magnetic and electromagnetic fields (1 Hz to 100 kHz)", Health Phys., vol. 99, no. 6, pp. 818-836, Dec. 2010.

[6] W. Zhang and C. C. Mi, "Compensation Topologies of High-Power Wireless Power Transfer Systems," in IEEE Transactions on Vehicular Technology, vol. 65, no. 6, pp. 4768-4778, June 2016.

[7] A. Safaee and K. Woronowicz, "Time-Domain Analysis of Voltage-Driven Series–Series Compensated Inductive Power Transfer Topology," in IEEE Transactions on Power Electronics, vol. 32, no. 7, pp. 4981-5003, July 2017.

[8] Y. Jiang, L. Wang, Y. Wang, J. Liu, X. Li and G. Ning, "Analysis, Design and Implementation of Accurate ZVS Angle Control for EV's Battery Charging in Wireless High Power Transfer," in IEEE Transactions on Industrial Electronics, vol. PP, no. 99, pp. 1-1.

[9] A. Berger, M. Agostinelli, S. Vesti, J. A. Oliver, J. A. Cobos and M. Huemer, "A Wireless Charging System Applying Phase-Shift and Amplitude Control to Maximize Efficiency and Extractable Power," in IEEE Transactions on Power Electronics, vol. 30, no. 11, pp. 6338-6348, Nov. 2015.

[10] K. Woronowicz, A. Safaee, T. Dickson, M. Youssef and S. Williamson, "Boucherot Bridge based zero reactive power inductive power transfer topologies with a single phase transformer," 2014 IEEE International Electric Vehicle Conference (IEVC), Florence, 2014, pp. 1-6.

[11] H. Kim et al., "Coil Design and Measurements of Automotive Magnetic Resonant Wireless Charging System for High-Efficiency and Low Magnetic Field Leakage," in IEEE Transactions on Microwave Theory and Techniques, vol. 64, no. 2, pp. 383-400, Feb. 2016.

[12] Wireless charging of electric and plug-in hybrid vehicles, Society of Automotive Engineers, SAE Std. J2954 [Online]. Available: http://standards.sae.org/wip/j2954/. [Accessed: Sept. 20, 2016].